Progress In Electromagnetics Research, PIER 100, 153–173, 2010

DESIGN OF THE COMPACT PARALLEL-COUPLED LINES WIDEBAND BANDPASS FILTERS USING IMAGE PARAMETER METHOD

C. S. Ye

Department of Electrical Engineering
Institute of Microelectronics Institute of Microelectronics
1 Ta-Hsueh Road, Tainan 701, Taiwan

Y. K. Su †

Department of Electrical Engineering & Advanced Optoelectronic Technology Center
National Cheng Kung University
1 Ta-Hsueh Road, Tainan 701, Taiwan

M. H. Weng

Medical Devices and Opto-electronics Equipment Department
Metal Industries Research & Development Center
3F, No. 88, Luke 5th Rd., Lujhu Township, Kaoshiung 82151, Taiwan

C. Y. Hung

Department of Electronics Engineering and Computer Sciences
Tung-Fang Institute of Technology
No. 110, Tung-Fung Road, Hunei Shiang
Kaohsiung County 829, Taiwan

R. Y. Yang

Department of Material Engineering
National Pingtung University of Science and Technology
No. 1, Syuefu Rd., Neipu Township, Pingtung County 912, Taiwan

Corresponding author: C. Y. Hung (goliro.goliro@msa.hinet.net).

† Also with Department of Electrical Engineering, Kun Shan University, 949 Dawan Road, Yongkang City, Tainan County 710, Taiwan.

Abstract—In this paper, the design of compact and high performance parallel coupled line wideband bandpass filter using image parameter method are proposed. The filter mainly comprising one-stage parallel coupled line and two open stubs are designed and implemented on commercial RT/Duroid 5880 substrate. The equivalent circuit of the proposed structure is initially derived by using the image parameter method. It is found that, the normalized bandwidth (NBW) of image impedance for the one-stage parallel coupled line has a relation to the electromagnetic (EM) simulated bandwidth. To further improve the selectivity, two open stubs are connected near the input/output (I/O) ports. The design procedures and their limitations are discussed in detail. The proposed filters are fabricated, measured and showing good characteristics of 87% fractional bandwidth as well as good insertion/return loss, flat group delay varies between 0.3–1.5 ns. High passband selectivity and wide stopband from 8–14 GHz are observed. The measured results are also having a good agreement with the simulated results.

1. INTRODUCTION

A small size, wide stopband and high selectivity microwave bandpass filter is widely used to enhance the performance of radio frequency (RF) front ends. Design of the bandpass filter is recently becoming stricter due to the increasing development of the Ultra-Wideband (UWB) systems, which attract great potential in various modern transmission systems, such as through-wall imaging, medical imaging, vehicular radar, indoor, and hand-held UWB systems, etc [1]. Being one of the important component blocks, efforts to develop wideband filters were made [2–14] in order to achieve such a specified fractional bandwidth (FBW, defined as 3 dB bandwidth over designed center frequency). In [2], a wideband equal-ripple filter with cascaded serial and shunt transmission-line sections produced a wide FBW of 54% and transmission zeros near the passband edges. However, this filter has several drawbacks, such as large size and complexity in configuration. In [3] and [4], parallel coupled line filters were constructed using a tight-coupling structure; however the reported FBW only achieved around 64% of the bandwidth. The parallel coupled-line microstrip filter fabricated on a printed circuit board usually has a relatively small bandwidth [15], which is mainly due to the fact that the reductions of strip width and strip spacing using conventional fabrication methods were limited. In [5–9], wideband filters having a wide FBW were achieved by using etched patterns in the ground plane or via holes. However, the structures with holes in the substrate or etched patterns

in the ground plane have the disadvantages, such as package problems, sensitivity and difficult realization in monolithic microwave integrated circuits (MMICs). Wideband bandpass filters using multiple-mode resonators to realize a fractional bandwidth of 100% have been reported by Zhu et al. [10–12]. However, the mentioned wideband filters still have some problems, such as 1arger size and slow rejection skirt. In [13], Hong et al. reported a novel UWB bandpass filter with pairs of transmission zeros by using five short-circuited stubs separated by nonredundant connecting lines. By introducing a cross-coupling between the feed lines, a pair of transmission zeros can be created at each side of the passband. However, most of above mentioned wideband filters had spurious passbands due to their structures with unequal even- and odd-mode phase velocity, or higher order resonant frequencies of the resonators. On the other hand, most of above mentioned wideband filters can not achieve the sharp attenuation skirt, wide-stopband and tunable bandwidth, simultaneously.

In a previous work, we proposed a compact parallel coupled lines wideband filter with a very high selectivity and a wide stopband [14]. However, the design procedure is not described in detail. The aim of this work is to develop a simple design procedure using the image parameter method to evaluate the bandwidth of the parallel coupled line with two open stubs. In this paper, compact and high-performance parallel coupled lines wideband filters achieve the wide stopband and high passband selectivity, simultaneously. The first challenge of using such a simple one-stage parallel coupled line for creating a wideband filter is to obtain an enough coupling strength, since the conventional synthesized method of the coupled line limits the FBW to 20% [15]. The second challenge is to obtain the high passband selectivity in this simple one-stage parallel coupled line structure. In Section 2, the image impedance of one-stage parallel coupled line connected with two open stubs is derived first. In Section 3, the design of parallel coupled line for achieving a wideband filter is discussed by varying the even/odd impedances to obtain different image impedance of one-stage parallel coupled line. Effect of the two open stubs on the passband performances and the selectivity is also analyzed. Finally, two filter samples, one is based on the one-stage parallel coupled line and other is a cascaded parallel coupled line, are designed, fabricated and measured to verify the theoretical concept.

2. THE IMAGE IMPEDANCE OF FILTER

The schematic layout and corresponding equivalent circuit for the proposed filter are shown in Figs. 1(a) and 1(b), respectively. It

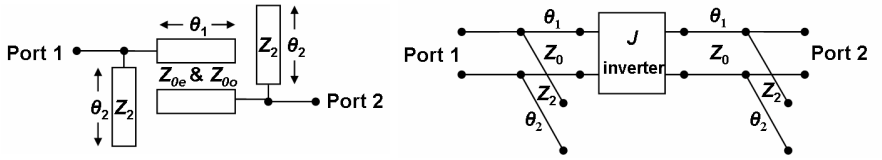

Figure 1. (a) Schematic layout and (b) equivalent circuit of the designed filter.

is composed of one-stage parallel coupled line and two open stubs connected near the input/output ports. In order to derive the image impedance of one-stage parallel coupled line with two open stubs, **ABCD** matrix is used [15]. The **ABCD** matrix of the coupled line is

$$M_c = \begin{bmatrix} \cos\theta_1 & jZ_0\sin\theta_1 \\ \frac{j\sin\theta_1}{Z_0} & \cos\theta_1 \end{bmatrix} \begin{bmatrix} 0 & -j/J \\ -jJ & 0 \end{bmatrix} \begin{bmatrix} \cos\theta_1 & jZ_0\sin\theta_1 \\ \frac{j\sin\theta_1}{Z_0} & \cos\theta_1 \end{bmatrix} \quad (1)$$

where Z_0 and θ_1 are the characteristic impedance and electrical length of the coupled line, respectively. J is the admittance inverter. Another, the **ABCD** matrix of the open stub, is

$$M_o = \begin{bmatrix} 1 & 0 \\ \frac{j\tan\theta_2}{Z_2} & 1 \end{bmatrix} \quad (2)$$

where Z_2 and θ_2 are the characteristic impedance and electrical length of open stub, respectively. The **ABCD** matrix of the equivalent circuit of the parallel coupled line with two open stubs can be obtained as

$$M_p = M_o M_c M_o \quad (3)$$

The admittance inverter J in **ABCD** matrix of M_c can be replaced by the even and odd mode characteristic impedances (Z_{0e}, Z_{0o}) of the coupled line according to Equation (4), [15]:

$$JZ_0 + \frac{1}{JZ_0} = \frac{Z_{oe} + Z_{oo}}{Z_{oe} - Z_{oo}} \quad (4)$$

where Z_{0e} and Z_{0o} are the even and odd mode characteristic. Therefore, the **ABCD** matrix of the coupled line becomes

$$M_c = \begin{bmatrix} \frac{Z_{oe}+Z_{oo}}{Z_{oe}-Z_{oo}}\cos\theta_1 & -\frac{j}{2}\left[\frac{4Z_{oe}Z_{oo}}{Z_{oe}-Z_{oo}}\frac{\cos^2\theta_1}{\sin\theta_1} - (Z_{oe}-Z_{oo})\sin\theta_1\right] \\ j\frac{2}{Z_{oe}-Z_{oo}}\sin\theta_1 & \frac{Z_{oe}+Z_{oo}}{Z_{oe}-Z_{oo}}\cos\theta_1 \end{bmatrix} \quad (5)$$

Hence, the **ABCD** matrix of the equivalent circuit of the parallel coupled line with two open stubs becomes

$$M_p = \begin{bmatrix} \frac{\tan\theta_2}{2Z_2}\left[\frac{4Z_{oe}Z_{oo}}{Z_{oe}-Z_{oo}}\frac{\cos^2\theta_1}{\sin\theta_1} - (Z_{oe}-Z_{oo})\sin\theta_1\right] + \frac{Z_{oe}+Z_{oo}}{Z_{oe}-Z_{oo}}\cos\theta_1 & -\frac{j}{2}\left[\frac{4Z_{oe}Z_{oo}}{Z_{oe}-Z_{oo}}\frac{\cos^2\theta_1}{\sin\theta_1} - (Z_{oe}-Z_{oo})\sin\theta_1\right] \\ j\left[\frac{\tan\theta_2}{Z_2}\frac{Z_{oe}+Z_{oo}}{Z_{oe}-Z_{oo}}\cos\theta_1 + \frac{2}{Z_{oe}-Z_{oo}}\sin\theta_1\right] & \frac{\tan\theta_2}{2Z_2}\left[\frac{4Z_{oe}Z_{oo}}{Z_{oe}-Z_{oo}}\frac{\cos^2\theta_1}{\sin\theta_1} - (Z_{oe}-Z_{oo})\sin\theta_1\right] \\ +\frac{j\tan\theta_2}{Z_2}\left\{\frac{\tan\theta_2}{2Z_2}\left[\frac{4Z_{oe}Z_{oo}}{Z_{oe}-Z_{oo}}\frac{\cos^2\theta_1}{\sin\theta_1} - (Z_{oe}-Z_{oo})\sin\theta_1\right] + \frac{Z_{oe}+Z_{oo}}{Z_{oe}-Z_{oo}}\cos\theta_1\right\} & +\frac{Z_{oe}+Z_{oo}}{Z_{oe}-Z_{oo}}\cos\theta_1 \end{bmatrix} \quad (6)$$

Since the proposed parallel coupled line with two open stubs is a symmetric circuit, the elements **A** and **D** in (6) are equal. It is noted that the image impedance Z_i is $\sqrt{\mathbf{AB}/\mathbf{CD}}$ [15]. Therefore the simplified expression for the image impedance Z_i is shown in (7)

$$Z_i = \sqrt{\frac{\mathbf{B}}{\mathbf{C}}} = \sqrt{\frac{\frac{1}{2}\left[(Z_{oe}-Z_{oo})\sin\theta_1 - \frac{4Z_{oe}Z_{oo}}{Z_{oe}-Z_{oo}}\frac{\cos^2\theta_1}{\sin\theta_1}\right]}{\frac{2\tan\theta_2}{Z_2}\frac{Z_{oe}+Z_{oo}}{Z_{oe}-Z_{oo}}\cos\theta_1 + \frac{2}{Z_{oe}-Z_{oo}}\sin\theta_1 + \frac{\tan^2\theta_2}{2Z_2^2}\frac{4Z_{oe}Z_{oo}}{Z_{oe}-Z_{oo}}\frac{\cos^2\theta_1}{\sin\theta_1} - \frac{\tan^2\theta_2}{2Z_2^2}(Z_{oe}-Z_{oo})\sin\theta_1}} \quad (7)$$

According to Equation (7), the electrical length $\theta 1$ and (Z_{0e}, Z_{0o}) of the coupled line, the electrical length θ_2 and characteristic impedance Z_2 of the open stub would affect the value of the image impedance Z_i. In next section, the derived image impedance Z_i is then used to analyze the parallel coupled line with two open stubs to understand how the above mentioned parameters influence the passband width of the parallel coupled line with or without the open stub.

3. ANALYSIS OF THE FILTER

Although the improved synthesized method of the coupled line used for multi-stages coupled line has been reported [4], the method is not suitable for the one-stage parallel coupled line. Therefore, we develop a novel method to decide the bandwidth of one-stage parallel coupled line by first estimating the bandwidth of image impedance Z_i.

It is known that the Z_{oe} and Z_{oo} are corresponding with the line width (w) and gap (g) of one-stage parallel coupled line. When

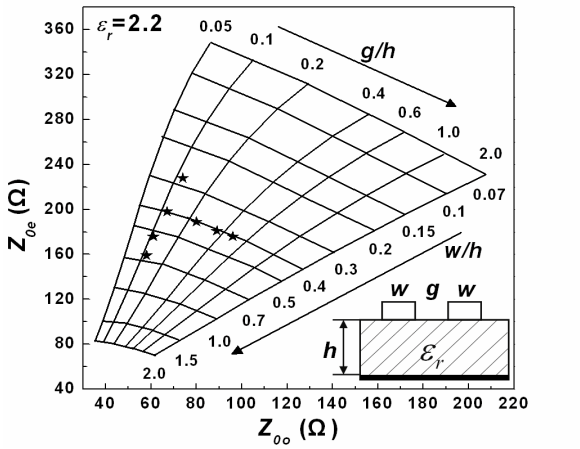

Figure 2. Even- and odd-mode characteristic impedance design graphs for one-stage parallel coupled lines. The substrate has $h = 0.787\,\text{mm}$ and $\varepsilon_r = 2.2$.

dielectric constant (ε_r) and thickness (h) of the substrate are known, the Z_{oe} and Z_{oo} can be calculated as functions of the strip line width (w) and coupling gap (g) of one-stage parallel coupled line by the conformal mapping method [16]. In this study, the used substrate is RT/Duroid 5880 with ε_r of 2.2 and h of 0.787 mm. By referring to [15, 16], we newly generated and plotted the corresponding design graphs versus different strip width (w/h) and coupling gaps (g/h), as shown in Fig. 2.

3.1. Design of One-stage Parallel Coupled Line without Open Stubs for Wide Bandwidth

For a one-stage parallel coupled line without open stubs, the electrical length θ_2 is set as 0 degree in Equation (7). Thus, the image impedance (Z_i) of the one-stage parallel coupled line is further simplified and expressed as

$$Z_i = \sqrt{(Z_{0e} - Z_{0o})^2 \csc^2\theta_1 - (Z_{0e} + Z_{0o})^2 \cot^2\theta_1} \tag{8}$$

According to (8), Z_i is real and positive, as $Z_{0e} > Z_{0o}$. When Z_i is equal to $\pm j\infty$ and $\text{Re}(Z_i)$ is equal to 0, a bandstop edge is introduced [14]. We then define a normalized bandwidth (NBW) of image impedance by subtracting right bandstop edge and left bandstop edge. It is then expected that by properly selecting the Z_{0e} and Z_{0o} of

one-stage parallel coupled line, the bandwidth scale can be tuned. To calculate the NBW, (Z_{0e}, Z_{0o}) pairs selecting from the horizontal star symbols along $w/h = 0.38$ line shown in Fig. 2 are first used. Namely, (Z_{0e}, Z_{0o}) with (198 Ω, 67 Ω), (189 Ω, 80 Ω), (181 Ω, 89 Ω) and (176 Ω, 96 Ω) are concentrated on the fixed strip width ($w/h = 0.38$) but with different coupling gaps ($g/h = 0.13$, 0.254, 0.38 and 0.51).

According to (8), the normalized $\theta_1/(\pi/2)$ for one-stage parallel coupled line is shown in Fig. 3(a). It is found that when (Z_{0e}, Z_{0o}) is (198 Ω, 67 Ω), (189 Ω, 80 Ω), (181 Ω, 89 Ω) and (176 Ω, 96 Ω), the estimated NBW are 68%, 56%, 48% and 40%, as shown in Fig. 3(a),

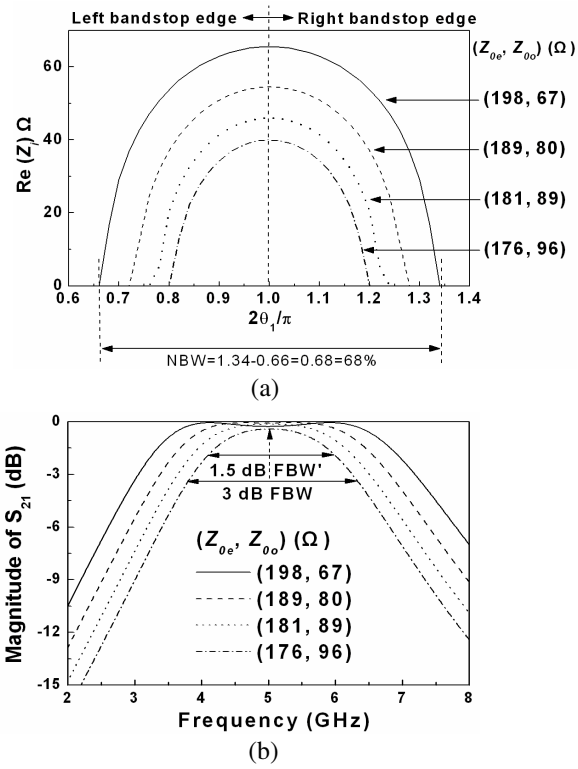

Figure 3. (a) The real part of the image impedance of one-stage parallel coupled line using the conditions of horizontal star symbols of Fig. 2 and (b) EM simulated frequency response of one-stage parallel coupled line of horizontal star symbols. The electrical length is $\theta_1 = 90°$ at center frequency $f_0 = 5$ GHz and $w/h = 0.38$. NBW and FBW are normalized bandwidth and fractional bandwidth, respectively, as defined in the text.

Table 1. NBW, FBW' and FBW as functions of the even and odd mode characteristic impedances of one-stage parallel coupled line structure, corresponding to the fixed strip width and different coupling gaps.

One-stage coupled line				
Z_{0e}, Z_{0o} (Ω)	198, 67	189, 80	181, 89	176, 96
w/h, *g/h*	0.38, 0.13	0.38, 0.254	0.38, 0.38	0.38, 0.51
Image Parameter method				
NBW (%)	68	56	48	40
Simulated prediction				
1.5 dB FBW' (%)	68.6	55	44.7	37.6
3 dB FBW (%)	81	67.7	57.5	50.3

respectively. Using the full wave electromagnetic (EM) simulator [17], the EM simulated frequency responses with different (Z_{0e}, Z_{0o}) pairs are shown in Fig. 3(b). It is found that at the same conditions, the 3 dB-FBW are 81%, 67.7%, 57.5% and 50.3%, respectively, but 1.5 dB-FBW' (defined as 1.5 dB bandwidth over the center frequency) are 68.6%, 55%, 44.7% and 37.6%, respectively, which are very similar to the estimated NBW. The correct values are listed in Table 1.

Second (Z_{0e}, Z_{0o}) pairs selecting from the vertical star symbols along $g/h = 0.13$ line shown in Fig. 2 are used to calculate the NBW. Namely, (Z_{0e}, Z_{0o}) with (228 Ω, 74 Ω), (198 Ω, 67 Ω), (176 Ω, 61 Ω) and (159 Ω, 58 Ω) are concentrated on the fixed coupling gap ($g/h = 0.13$) but with different strip widths (w/h = 0.254, 0.38, 0.51 and 0.635). The normalized $\theta_1/(\pi/2)$ for one-stage parallel coupled line is shown in Fig. 4(a). It is found that when (Z_{0e}, Z_{0o}) is (228 Ω, 74 Ω), (198 Ω, 67 Ω), (176 Ω, 61 Ω) and (159 Ω, 58 Ω), the estimated NBW is 72%, 68%, 68% and 64%, as shown in Fig. 4(a), respectively. Similarly, the EM simulated frequency responses, as shown in Fig. 4(b), indicate that the 3 dB-FBW are 89%, 81%, 77.6% and 74%, respectively, but 1.5 dB-FBW' are 78%, 68.6%, 64% and 58%, respectively, which are also very similar to the estimated NBW. The correct values are listed in Table 2. Above two results indicate the NBW calculated from the image parameter has a corresponding relation with the 1.5 dB-FBW' estimated form the EM simulation.

Since 3 dB-FBW is used more frequently, the statistics chart obtained by taking the 3 dB-FBW divided by NBW is shown in Fig. 5. It varies between 1.14–1.2. Moreover, if the length of the one-stage parallel coupled line is close to quarter wavelength, the coupled line

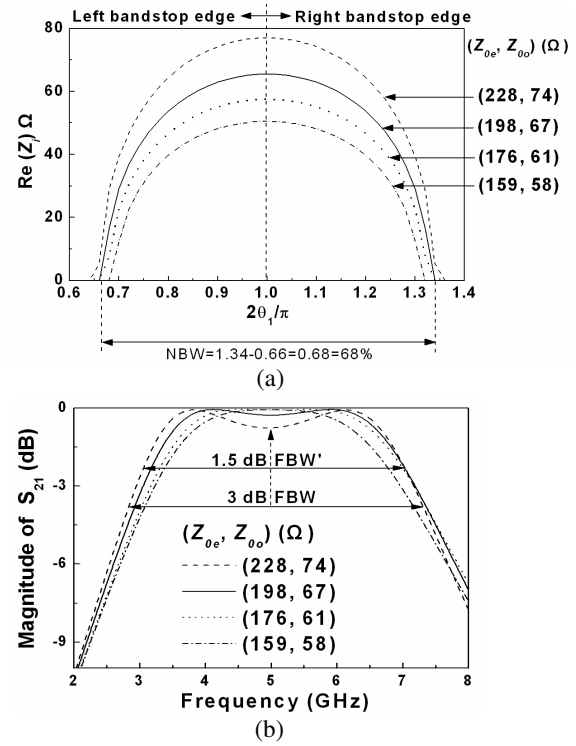

Figure 4. (a) The real part of the image impedance of one-stage parallel coupled line using the conditions of vertical star symbols of Fig. 2 and (b) EM simulated frequency response of one-stage parallel coupled line of vertical star symbols. The electrical length is $\theta_1 = 90^\circ$ at center frequency $f_0 = 5\,\text{GHz}$ and $g/h = 0.13$.

becomes very compact. The result indicates by properly selecting the Z_{0e} and Z_{0o} of one-stage parallel coupled line, the wide bandwidth can be estimated. Additionally, from the above analysis, (Z_{0e}, Z_{0o}) of $(228\,\Omega,\ 74\,\Omega)$ has a larger NBW of 72%, but the EM simulated frequency response displays the resonant modes are slightly separated. Thus this condition does not suit to design smooth passband of filter. (Z_{0e}, Z_{0o}) of $(198\,\Omega,\ 67\,\Omega)$ has a 3 dB-FBW of 81% is suitable. Although the FBW is large enough, however, the attenuation rates of lower and higher passband edges are still slow, causing the poor selectivity. Therefore, to create some attenuation poles near the passband edges to improve the passband selectivity is needed.

Table 2. NBW, FBW' and FBW as functions of the even and odd mode characteristic impedances of one-stage parallel coupled line structure, corresponding to the fixed coupling gap and different strip widths.

One-stage coupled line				
Z_{0e}, Z_{0o} (Ω)	228, 74	198, 67	176, 61	159, 58
w/h, *g/h*	0.254, 0.13	0.38, 0.13	0.51, 0.13	0.635, 0.13
Image Parameter method				
NBW (%)	72	68	68	64
Simulated prediction				
1.5 dB FBW' (%)	78	68.6	64	58
3 dB FBW (%)	89	81	77.6	74

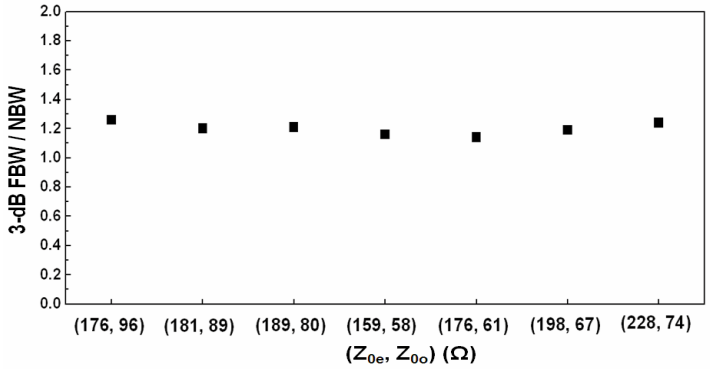

Figure 5. The statistics chart of the ratio of the 3 dB-FBW/NBW.

3.2. Controlling the Attenuation Pole by θ_2/θ_1 Ratio

In past, open stubs are usually used to create a notch band or suppress the harmonics [18, 19]. In this study, the use of open stubs in the proposed structure not only improves the passband edge skirt but also provide suppression effect, simultaneously. Fig. 6 depicts the primary structure of the proposed filter using a one-stage parallel coupled line and two open stubs connected near the input/output (I/O) ports. Following section will analyze the effect of the structural parameters of the open stubs on the passband performances.

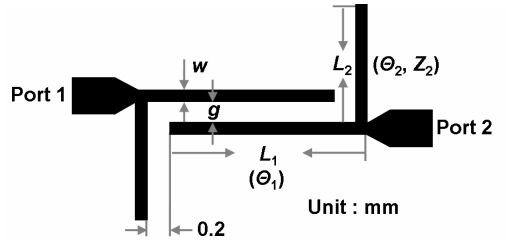

Figure 6. Practical layout of the designed wideband filter designed on a 0.787-mm-thick substrate with a dielectric constant of 2.2.

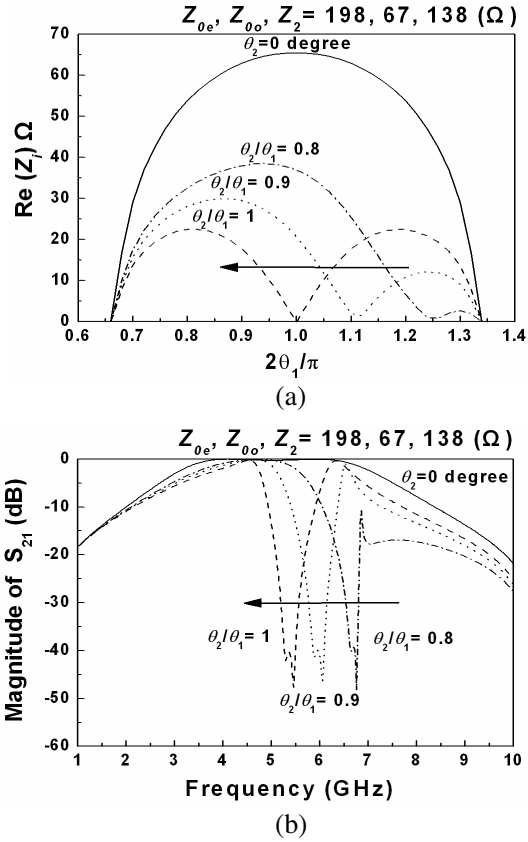

Figure 7. (a) The real part of the image impedance of one-stage parallel coupled line and (b) the EM simulated response as a function of θ_2/θ_1 ratio.

3.2.1. θ_2/θ_1 Ratio ≤ 1

For a one-stage parallel coupled line with open stubs, the electrical length θ_2 is not 0 degree in Equation (7). Fig. 7(a) plots the real part of the image impedance, corresponding to NBW, according to Equation (7) as a function of θ_2/θ_1 ratio ≤ 1. When θ_2/θ_1 is 0.8, the bandstop node is produced at 1.25, causing the deep right bandstop edge. When θ_2/θ_1 is 0.9, the bandstop node is shifted to 1.1, causing two asymmetry passband regions. When θ_2/θ_1 is 1, the bandstop node is shifted to 1, causing two almost symmetry passband regions. Fig. 7(b) plots the EM simulated response as a function of θ_2/θ_1 ratio ≤ 1. The length of one-stage parallel coupled line is close to quarter wavelength at 5 GHz and has a strip width (w/h) of 0.38 and coupling gap (g/h) of 0.13. The attenuation pole shifts from 6.68 to 5.36 GHz by increasing the θ_2/θ_1 ratio as 0.8 to 1. From the above discussion, the $\theta_2/\theta_1 < 1$ is not suitable for creating a proper attenuation poles near the passband edges due to the short physical length of the open stub [20]. However, it is clearly observed that the EM simulated performers are analogous with the performances from the image parameter method. It is then expected that for any pairs of (Z_{0e}, Z_{0o}), two attenuation poles near the lower and higher passband edges can be realized by optimum selection of θ_2/θ_1.

3.2.2. θ_2/θ_1 Ratio > 1

To improve left and right passband edges at the same time, the fundamental and spurious bandstop nodes of the open stub should be properly selected. The first bandstop node is used in the left passband edge and second bandstop node is used in the right passband edge by properly selecting the θ_2/θ_1 ratio from 1.84 to 2.2.

The real part of the image impedance, corresponding with the NBW, as shown in Fig. 8(a). When θ_2/θ_1 is 1.84, the second bandstop node is not matched for the right bandstop edge due to the smaller θ_2/θ_1 ratio, causing poor selectivity in right passband edge. While θ_2/θ_1 is 2.2, the first bandstop node is not matched for the left bandstop edge due to the larger θ_2/θ_1 ratio, causing poor selectivity in left passband edge. By properly selecting θ_2/θ_1 as 2.03, the first and second bandstop nodes match for the left and the right bandstop edges, respectively. EM simulated responses of the filter in Fig. 8(b) shows the similar behaviors analogous to the Fig. 8(a). It is observed that when θ_2/θ_1 is 2.2, 2.03 and 1.84, the first attenuation pole frequency (f_n) is 2.4 GHz, 2.63 GHz and 2.89 GHz and the second attenuation pole frequency (f_{n1}) is 7.18 GHz, 7.83 GHz and 8.59 GHz, respectively. As found in Fig. 8(a), a satisfied passband at center

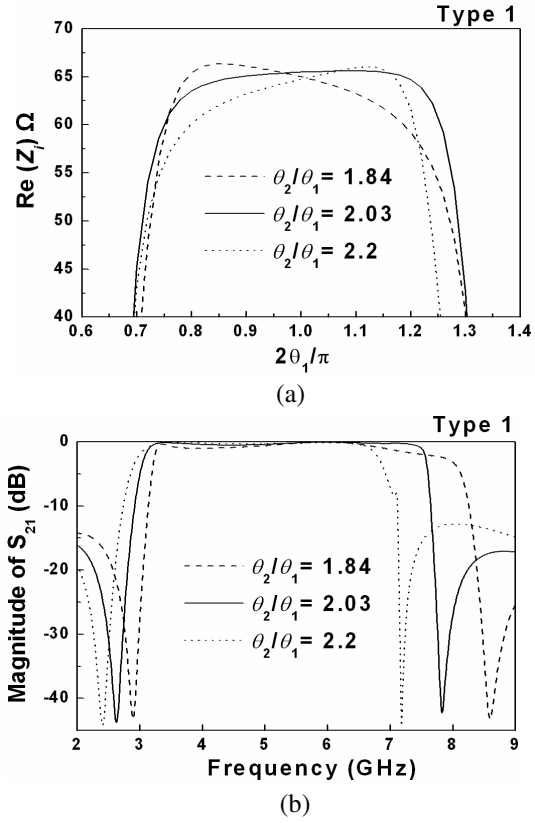

Figure 8. (a) The real part of the image impedance of one-stage parallel coupled line and (b) the EM simulated response as θ_2/θ_1 ratio of 1.84, 2.03 and 2.2. The one-stage parallel coupled line as the (Z_{0e}, Z_{0o}) is (198 Ω, 67 Ω), θ_1 is $\pi/2$ and Z_2 is 138 Ω.

frequency f_0 = 5.3 GHz would have a bandwidth of 3.05–7.58 GHz (FBW = 85%) under the proper θ_2/θ_1 ratio of 2.03.

Except the improvement of the attenuation skirt near the passband edge, an interesting phenomenon in compensating the energy of the passband edge by using the open stub connecting to the coupled lines is also found. Fig. 9(a) shows the real part of the image impedance of one-stage parallel coupled line as θ_2/θ_1 ratio of 2.03 and θ_2 = 0 degree. With addition of the open stubs, the real part of the image impedance shows a flat value of 60 Ω and the sharp attenuation rate for the two bandstop nodes. The result is also confirmed by the EM simulated filter response as θ_2/θ_1 ratio of 2.03 and θ_2 = 0 degree,

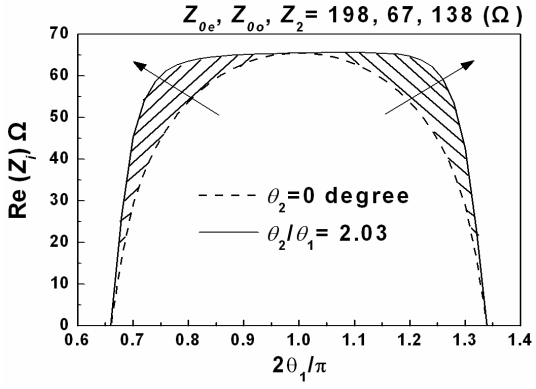

(a)

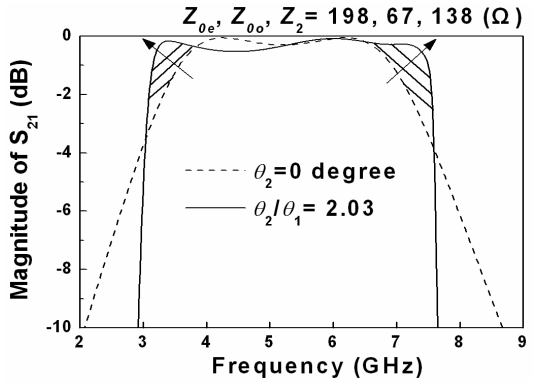

(b)

Figure 9. (a) The real part of the image impedance of one-stage parallel coupled line and (b) the EM simulated response as θ_2/θ_1 ratio of 2.03 and $\theta_2 = 0$ degree.

as shown in Fig. 9(b). After adding the proper open stubs with the θ_2/θ_1 ratio of 2.03, the attenuation rates are enhanced since the attenuation poles at frequency 2.63 GHz (f_n) and 7.83 GHz ($f_{n1} = 3f_n$) are appeared in the lower and higher passband edges, respectively. This result indicates a very high selectivity with 97 dB/GHz and 220 dB/GHz attenuation slopes in lower and higher passband edges, respectively. Note that, a flat passband ripple as well as the passband selectivity is much improved since the energies are compensated from the low attenuation areas to the oblique-line area of passband edges, as clearly observed in Fig. 9(b).

3.3. Effect of Impedance (Z_2) of the Open Stub on the Performances

According to Equation (7), the characteristic impedance Z_2 would effect the value of the image impedance can change the Z_i, thus the NBW would also be influenced. Real part of the image impedance according to Equation (7) and EM simulated responses of one-stage parallel coupled line filter with several values of Z_2 are shown in Fig. 10. It is found that Z_2 also slightly affects the attenuation slopes of two passband edges. When Z_2 achieves 138 Ω, the attenuation slopes in two passband edges are much improved. In the range of 2.5–3.5 GHz,

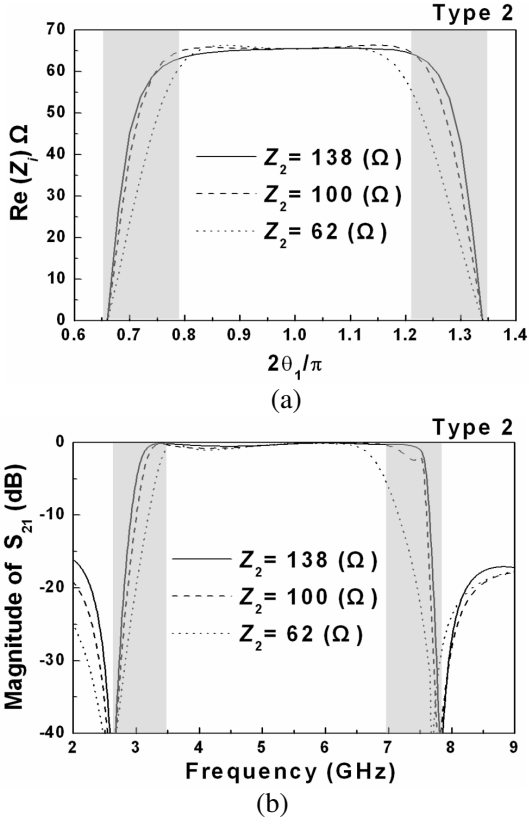

Figure 10. (a) The real part of the image impedance of one-stage parallel coupled line and (b) the EM simulated response as Z_2 value of 62 Ω, 100 Ω and 138 Ω. The (Z_{0e}, Z_{0o}) of one-stage parallel coupled line is (198 Ω, 67 Ω) and θ_2/θ_1 is 2.03.

the attenuation slope is 52 dB/GHz, 80 dB/GHz and 98 dB/GHz when Z_2 is 62 Ω, 100 Ω and 138 Ω, respectively. It is also found that the performances estimated using the image parameter method and the EM simulation tool are very similar and analogous, as observed in prior section.

3.4. Limits of the Design of FWB Using the Open Stubs

Limits of FWB the proposed filter using the open stub have been discussed in our previous work [14]. Since the open stub creates the first attenuation pole at f_n and the second attenuation pole frequency f_{n1} (at $3f_n$) to be used in the lower passband edge and the higher passband edge, respectively, the bandwidth of proposed design is limited to $2f_n$. Therefore, the FBW will be limited theoretically to 100%. Even FBW will be further limited by material properties but the ratio of f_{n1}/f_n can be further enlarged by using the stepped-impedance (SIR) open stub.

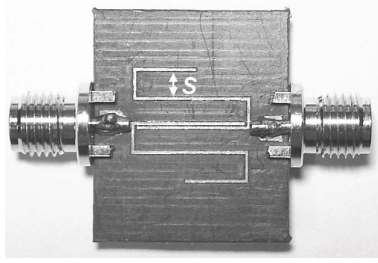

(a)

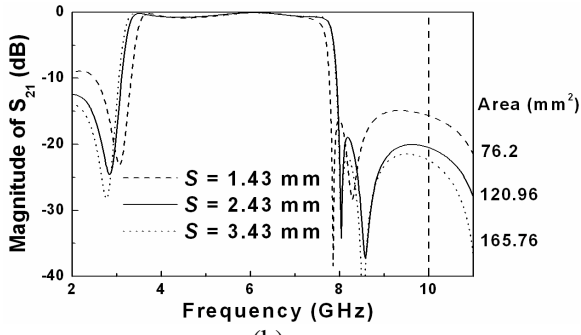

(b)

Figure 11. (a) Picture and (b) circuit area and attenuation level as a function of folding distance "S" of open stubs. The physical size parameters of the designed filter are: $w = 0.3$ mm, $S = 2.43$ mm, $L_1 = 10.7$ mm and $L_2 = 21.7$ mm.

4. EXPERIMENTAL RESULTS AND DISCUSSION

Using the optimized structural parameters, filter sample with the (Z_{0e}, Z_{0o}) of $(198\,\Omega, 67\,\Omega)$, θ_2/θ_1 of 2.03 and Z_2 of $138\,\Omega$ is fabricated on the RT/Duroid 5880 substrate and measured by an network analyzer HP 8510C to coupled line filter, as shown in Fig. 11(a). To achieve a compact size, the two tapped open stubs are folded. The effect of the folding distance (S) on the filter performance is first EM simulated and shown in Fig. 11(b). It is found that the different S values do not affect the passband performances but actually perturb the attenuation level of the stopband as well as the circuit area, simultaneously. When a small S value (1.43 mm) is used, the filter can have a small circuit area as $76.2\,\text{mm}^2$, but the attenuation level is $-15.65\,\text{dB}$ at 10 GHz due to the coupling between the folding open stubs and the parallel coupled line. Although S of 3.43 mm can have a small attenuation level of $-22.4\,\text{dB}$ at 10 GHz, but the filter size is as large as $165.76\,\text{mm}^2$. After trade-off using EM simulation, S of 2.43 mm is used in this paper. The whole size of the fabricated one-stage parallel coupled line filter is $10.8\,\text{mm} \times 11.2\,\text{mm}$, i.e., approximately $0.27\lambda_g$ by $0.28\lambda_g$, where λ_g is the guided wavelength at the center frequency. Fig. 12(a) shows the simulated and measured results. The measured results show a center frequency f_0 of 5.55 GHz, a very low insertion loss of $0.5 \pm 0.2\,\text{dB}$, a wide bandwidth of 3.13–7.96 GHz (FBW = 87%) and a wide stopband rejection greater than 15 dB from 8–14 GHz. The attenuation poles are clearly observed in the lower passband edge at 2.86 GHz with $-24\,\text{dB}$ attenuation and in the higher passband edge at 8.14 GHz with $-29\,\text{dB}$ attenuation. The group delay shown in Fig. 12(b) is obtained by taking the derivative of the measured and simulated phase and varies between 0.15–1.8 ns in whole passband.

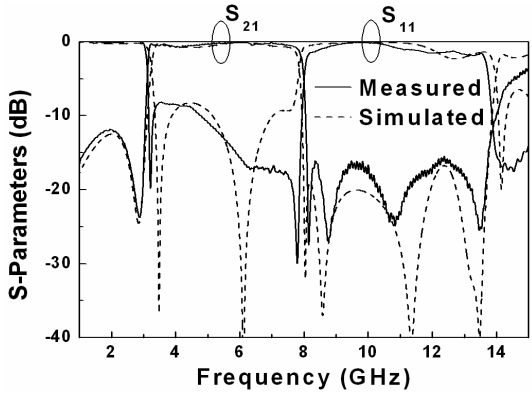

(a)

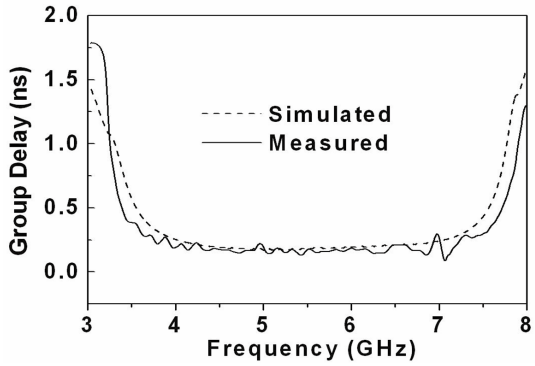

(b)

Figure 12. (a) Simulated and measured frequency response of the designed filter and (b) the group delay over the entire passband. The physical size parameters of the designed filter are: $w = 0.3\,\text{mm}$, $S = 2.43\,\text{mm}$, $L_1 = 10.7\,\text{mm}$ and $L_2 = 21.7\,\text{mm}$.

Figure 13(a) shows the fabricated filter cascaded with two filter units. It is believed that the stopband rejection level can be further improved by cascading more stages of coupled lines directly. The structural parameters of the second samples by cascading two-stage parallel coupled line filter are the same with the first one. Fig. 13(b) shows the simulated and measured results. The measured results have a center frequency f_0 of 5.55 GHz, a very low insertion loss of $1 \pm 0.3\,\text{dB}$ and a wide bandwidth of 3.22–7.87 GHz (FBW = 84%). The attenuation poles are clearly observed in the lower passband edge at 3 GHz with $-51\,\text{dB}$ attenuation and in the higher passband edge at 8.14 GHz with $-37\,\text{dB}$ attenuation. The measured and simulated group delay shown in Fig. 13(c) varies between 0.3–2.0 ns in whole passband. Such high attenuation slope in the passband edges is hard to be implemented on the commercial substrate, except on the superconductor substrate or high order dielectric resonators. The measured results actually verify the possibility of the proposed design concept. Although the measured results are somewhat different than the simulated results in the higher band, it can be considered as fabrication error, but the proposed filter still shows a good potential for the broadband communication.

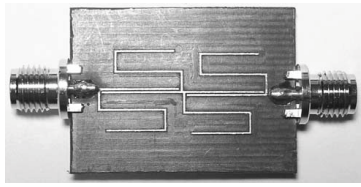

(a)

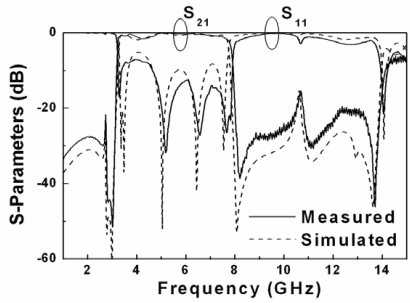

(b)

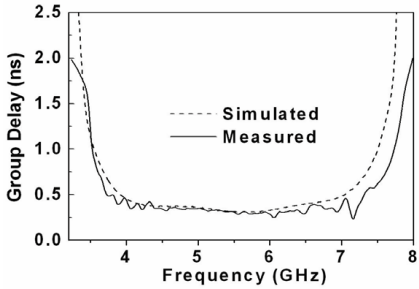

(c)

Figure 13. (a) Picture and (b) simulated and measured frequency responses of the cascaded filter and (c) the measured group delay over the entire passband.

5. CONCLUSION

In this paper, we have developed a simple design procedure using the image parameter method to evaluate the bandwidth of the parallel coupled line with two open stubs and then two wideband filters are designed and fabricated to experimentally verify the theoretical design concept. It is found the normalized bandwidth (NBW) calculated using real part of image impedance of the one-stage parallel coupled line has a similar and analogous behavior with the EM simulated bandwidth. In addition, two open stubs are connected near the input/output (I/O) ports to further improve the passband selectivity. Two filter samples,

one is based on the one-stage parallel coupled line and other is a cascaded parallel coupled line, are designed, fabricated and measured, showing good characteristics including the 3-dB FBW around 87%, a very low insertion, a wide stopband from 8–14 GHz and a very high selectivity due to two attenuation poles near the passband edges created by the open stubs.

ACKNOWLEDGMENT

Financial support of this study by the National Science Council of the Republic of China under grant no. NSC 97-2218-E-272-002 is greatly appreciated.

REFERENCES

1. El-Fishawy, N. A., M. Shokair, and W. Saad, "Proposed MAC protocol versus IEEE 802.15.3a for multimedia transmission over UWB networks," *Progress In Electromagnetics Research B*, Vol. 2, 189–206, 2008.
2. Chang, D. C. and C. W. Hsue, "Wide-band equal-ripple filters in nonuniform transmission lines," *IEEE Trans. Microw. Theory Tech.*, Vol. 50, No. 4, 1114–1119, Apr. 2002.
3. Chen, C. C., J. T. Kuo, M. Jiang, and A. Chin, "Study of parallel coupled-line microstrip filter in broadband," *Microw. Opt. Tech. Lett.*, Vol. 48, No. 2, 373–375, Feb. 2006.
4. Chin, K. S., L. Y. Lin, and J. T. Kuo, "New formulas for synthesizing microstrip bandpass filters with relatively wide bandwidths," *IEEE Microw. Wireless Compon. Lett.*, Vol. 14, No. 5, 231–233, May 2004.
5. Shobeyri, M. and M. H. Vadjed-Samiei, "Compact ultra-wideband bandpass flter with defected ground structure," *Progress In Electromagnetics Research Letters*, Vol. 4, 25–31, 2008.
6. Naghshvarian-Jahromi, M. and M. Tayarani, "Miniature planar UWB bandpass filters with circular slots in ground," *Progress In Electromagnetics Research Letters*, Vol. 3, 87–93, 2008.
7. Wei, F., P. Chen, L. Chen, and X. W. Shi, "Design of a compact UWB bandpass filter with defected ground structure," *Journal of Electromagnetic Waves and Applications*, Vol. 22, No. 13, 1783–1790, 2008.
8. Wu, B., X. Lai, T. Su, and C. H. Liang, "Wideband cross coupled filter using split-ring resonator defected ground structure,"

Journal of Electromagnetic Waves and Applications, Vol. 22, Nos. 11–12, 1631–1638, 2008.

9. An, J., G.-M. Wang, W.-D. Zeng, and L.-X. Ma, "UWB flter using defected ground structure of Von Koch fractal shape slot," *Progress In Electromagnetics Research Letters*, Vol. 6, 61–66, 2009.
10. Zhu, L., S. Sun, and W. Menzel, "Ultra-wideband (UWB) bandpass filters using multiple-mode resonator," *IEEE Microw. Wireless Compon. Lett.*, Vol. 15, No. 11, 796–798, Nov. 2005.
11. Sun, S. and L. Zhu, "Capacitive-ended interdigital coupled lines for UWB bandpass filters with improved out-of-band performances," *IEEE Microw. Wireless Compon. Lett.*, Vol. 16, No. 8, 440–442, Aug. 2006.
12. Li, R. and L. Zhu, "Compact UWB bandpass filter using stub-loaded multiple-mode resonator," *IEEE Microw. Wireless Compon. Lett.*, Vol. 17, No. 1, 40–42, Jan. 2007.
13. Shaman, H. and J. S. Hong, "A novel ultra-wideband (UWB) bandpass filter (BPF) with pairs of transmission zeroes," *IEEE Microw. Wireless Compon. Lett.*, Vol. 17, No. 2, 121–123, Feb. 2007.
14. Hung, C. Y., M. H. Weng, R. Y. Yang, and Y. K. Su, "Design of the compact parallel coupled wideband bandpass filter with very high selectivity and wide stopband," *IEEE Microw. Wireless Compon. Lett.*, Vol. 17, No. 7, 510–512, Jul. 2007.
15. Pozar, D. M., *Microwave Engineering*, Wiley, Hoboken, 2005.
16. Kirschning, M. and R. H. Jansen, "Accurate wide-range design equations for the frequency-dependent characteristic of parallel coupled microstrip lines," *IEEE Trans. Microw. Theory Tech.*, Vol. 32, No. 1, 83–90, Jan. 1984.
17. Zeland Software, Inc., IE3D Simulator, 1997.
18. Hsieh, L. H. and K. Chang, "Compact, low insertion-loss, sharp-rejection, and wide-band microstrip bandpass filters," *IEEE Trans. Microw. Theory Tech.*, Vol. 51, No. 4, 1241–1246, Apr. 2003.
19. Tu, W. H. and K. Chang, "Compact second harmonic-suppressed bandstop and bandpass filters using open stubs," *IEEE Trans. Microw. Theory Tech.*, Vol. 54, No. 6, 2497–2502, Jun. 2006.
20. Hung, C. Y., M. H. Weng, Y. K. Su, and R. Y. Yang, "A simple method to design a compact and high performance wideband filter," *Microw. Opt. Tech. Lett.*, Vol. 49, No. 4, 822–824, Apr. 2007.